FABRICATION OF AlGaAs/GaAs CASCADE SOLAR CELL BY LPE

S. M. Bedair
Research Triangle Institute
Research Triangle Park, North Carolina

SUMMARY

Multi-junction, variable bandgap cascade solar cells offer the potential of achieving significantly higher conversion efficiencies than single junction cells and are therefore attractive candidates for future terrestrial and space applications. This paper reports on the successful fabrication of high efficiency cascade solar cells in the Al-Ga-As system.

INTRODUCTION

Stacking two or more photovoltaic junctions in electrical and optical series results in higher conversion efficiency since each junction can be tailored to respond more efficiently to a smaller range of photon energies. An efficiency of about 30% has been predicted for a two junction cascade cell having the optimum bandgap values (1,2).

A number of III-V materials systems are currently being considered for use in fabricating cascade solar cells (3). The Al-Ga-As system (4) is attractive from a developmental standpoint since it employs a proven materials system that is closely lattice matched throughout its compositional range. This system (figure 1) employs a GaAs low bandgap cell and 1.9 eV AlGaAs high bandgap cell connected by an AlGaAs tunnel junction. Although this cell does not posses the optimum bandgap values, an efficiency of 25% is predicted at 300°K under AM0, 1 sun illumination.

Experimental and Results

The cascade cell shown in figure 1 is a seven-layer structure epitaxially grown on a GaAs substrate ($n \simeq 10^{18} cm^{-3}$). It consists of two diffused GaAs and $Al_{0.35}Ga_{0.65}As$ junctions which are electrically connected by an $Al_{0.35}Ga_{0.65}As$ tunnel junction. Junction depths are in the 0.5 to 1 μm range as determined by SEM measurements. Table 1 shows the composition, doping concentration and thickness of each layer. Beryllium was chosen as the p^+-dopant for the window layers of both junctions because of its low vapor pressure, necessary for the multiwell LPE growth technique. Also higher doping concentrations can be more easily achieved in high bandgap AlGaAs with Be. Doping characteristics and electrical properties of Be-doped AlGaAs have been reported elsewhere (5).

Several problems are associated with using Be as an impurity. First, it is a toxic material and several precautions have to be considered in its handling. Second, because it is very reactive successful use of Be is limited to LPE systems that are completely oxygen free. The third problem is its very high distribution coefficient; thus very small amounts on the order of micrograms are used in the LPE melts.

For $Al_xGa_{1-x}As$ in the direct bandgap region ($0 < x < 0.37$) it is very hard to achieve doping concentrations lower than the mid 10^{18} range when using Be. However, for $x > 0.5$ doping concentrations in the high $10^{17}cm^{-3}$ and low $10^{18}cm^{-3}$ regions can be routinely achieved (5). Thus, as shown in Table I, the $Al_xGa_{1-x}As$ window layer, which is used as a source for Be diffusion into the GaAs junction, was chosen such that $x = 0.7$. This then allowed the carrier concentration in the p-side of the GaAs junction to be limited to the high $10^{17}cm^{-3}$ range, thereby maintaining a good electron diffusion length.

Junctions formed by Be diffusion in $Al_xGa_{1-x}As$ ($0 < x < 0.37$) grown on GaAs substrates have been characterized by excellent electrical properties as shown in figure 2 for $Al_{0.35}Ga_{0.65}As$. Open circuit voltages in the 1 to 1.3 V range have been obtained both at AM0 and AM2 at 1 sun. The best fill factors have varied from 0.8 to 0.84. Short circuit current densities at AM0 have varied from 8 to 13 mA/cm^2 (based on active device area) without an antireflection coating. This cell had an AM0, 1 sun efficiency of ≈10% without an antireflection coating. Figure 3 shows the quantum efficiency of an $Al_{0.3}Ga_{0.7}As$ cell without an antireflection coating. A quantum efficiency up to about 0.7 indicates excellent current collection for this high bandgap cell. These results have been obtained by minimizing the window layer thickness and optimizing the junction depth.

The AlGaAs tunnel junctions have been fabricated using Ge and Te as the p^+ and n^+ dopants, respectively (6). Both impurities have the low diffusion coefficients in GaAs and AlGaAs as required for abrupt tunnel junction formation. Several difficulties have resulted from the use of Te in the tunnel junction. Tellurium tends to form compounds (7) both with Ga and Al such as Al_2Te_3, GaTe, etc. These compounds form precipitates that create and propagate lattice defects in the top AlGaAs cell. Although the phase diagram of the Al-Ga-As-Te quaternary alloy has not been studied, growth at temperatures above 900°C has been found to eliminate the formation of these unwanted compounds. However, this temperature is too high to obtain the necessary abrupt doping profile for the tunnel junction. This difficulty was significantly reduced in the present study by performing the growths at 800°C according to the following procedure (8). Gallium and GaAs were first baked together at 900°C two hours and then cooled to room temperature before the addition of Te and Al to the melt. Upon reheating to the deposition temperature of 800°C and performing the growth, a smooth, specular AlGaAs epitaxial layer was obtained. A possible explanation is that when the prebaked (saturated) GaAs melt is quenched to room temperature, GaAs crystallites are formed. These solid crystallites in the melt may act as nucleation sites for the Te compounds during the process of melt saturation at 800°C. It appears that the GaAs crystallites are of sufficient concentration to trap most of the Te compound that will otherwise disturb the epitaxial layer. Defects propagated into the top AlGaAs junction from the tunnel junction have

been further reduced through the use of a rather thick n-AlGaAs layer separating the two structures.

The terminal I-V characteristic of a complete cascade cell consisting of an AlGaAs top cell and connecting junction and a GaAs bottom cell is shown in figure 4. Open circuit voltages in the range of 1.9 to 2.15 V have been obtained under 1 sun, AM0 illumination. Short circuit current densities up to 12 and 13 mA/cm^2 (based on active device area) have been obtained at AM1 and AM0, respectively, without antireflection coatings. This has been achieved by close matching of the currents generated by each cell (each cell absorbs one half of the solar spectrum). These current densities are equal to one half of the J_{sc} reported for the best GaAs single-junction solar cell. The best cascade cell fabricated to date had efficiency values of 15.2% at AM0 and 16.4% at AM1 without AR coating and 19.5% at AM0 and 21% when corrected for losses due to surface reflectance. The spectral response of the total cascade structure is shown in figure 5. The dip between 0.65 and 0.7 μm occurs at the wavelength where the GaAs junction starts to cut off due to photon absorption by the tunnel junction and the AlGaAs junction. A flat response is desired for maximum quantum and power conversion efficiencies.

At high concentrations (≈30 suns) the tunnel junction starts to show some undesirable effects depending on its abruptness and bandgap. High series resistance and in some cases non-ohmic behavior have been observed. This has resulted in a poor fill factor and a drop in efficiency of the total structure. In cases when a high-quality tunnel junction is present between the two cells, a negative resistance region is observed in the I-V characteristics shown in figure 6. Here the short-circuit current density resulting from high solar concentration has exceeded the peak current value (I_p) of the AlGaAs tunnel junction (8).

CONCLUSION

High efficiency AlGaAs/GaAs cascade solar cells have been fabricated. The conditions for current matching between the junctions have been met by optimizing the cell parameters in this structure. Efficiencies of 15.2% at AM0 and 16.4% at AM1 have been achieved without AR coating which corresponds to 19.5% at AM0 and 21% at AM1 when corrections for reflectance losses are included.

REFERENCES

1. Lamorte, M. F.; and Abbott, D. H.: Proc. 13th Photovoltaic Specialists Conference, 874 (1978).

2. Moon, R. L.; James, L. W.; Vander Plas, T. O.; Antypas, G. A.; and Chai, Y.: Proc. 13th Photovoltaic Specialists Conference, 859 (1978).

3. Bedair, S. M.; Phatak, S. B.; and Hauser, J. R.: IEEE Elect. Devices, ED-27, 822 (1980).

4. Bedair, S. M.; Lamorte, M. F.; and Hauser, J. R.: Appl. Phys. Lett. 34, 38 (1979).

5. Fujita, S.; Bedair, S. M.; Littlejohn, M. A.; and Hauser, J. R.: accepted for publication, J. Appl. Phys.

6. Bedair, S. M.: J. Appl. Phys. 50, 7267 (1979).

7. Wagner, W. R.: J. Appl. Phys. 49, 173 (1978).

8. Bedair, S. M.: J. Appl. Phys. 51, 3937 (1980).

Table I. Composition, Doping Level and Thickness of Each Layer

Layer	n	p	Thickness (μm)	AlAs%
n-GaAs	10^{17}		4	
p^+-AlGaAs(window)		$1x10^{18}$(Be)	0.5	70
p^+-AlGaAs		$\simeq 5x10^{18}$(Ge)	0.4	35
n^+-AlGaAs	$\simeq 5x10^{18}$(Te)		0.4	35
n-AlGaAs	10^{17}		5	35
p^+-AlGaAs(window)		$2x10^{18}$(Be)	0.2	90

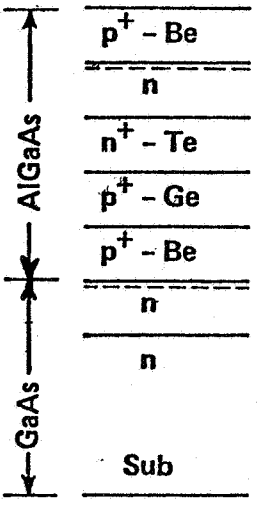

Figure 1. Structure of AlGaAs/GaAs Cascade Solar Cell

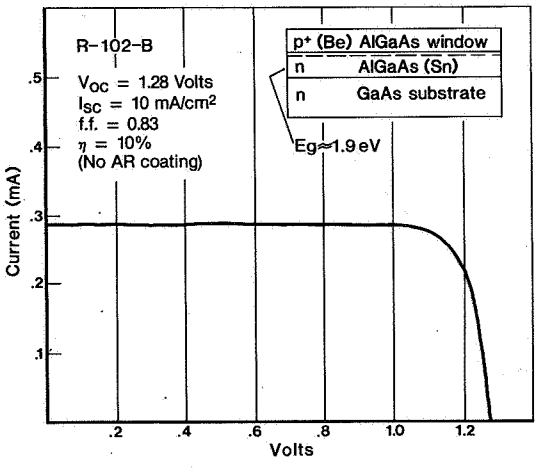

Figure 2. V-I Characteristics for AlGaAs Top Cell at AM0, 1 sun

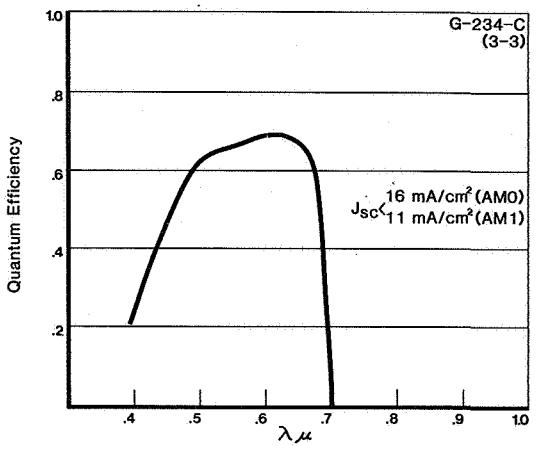

Figure 3. Quantum Efficiency of $Al_{0.3}Ga_{0.7}As$ p-n Junction Without AR Coating

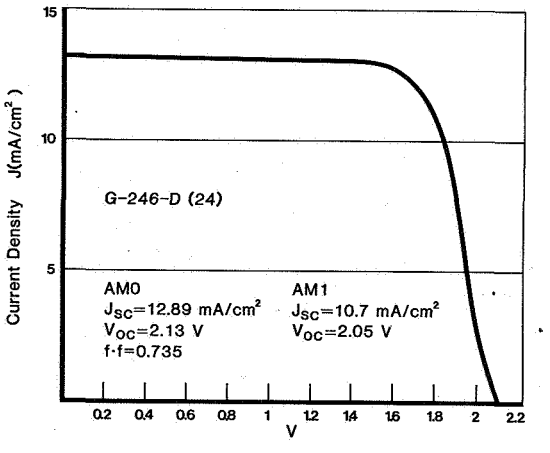

Figure 4. V-I Characteristics for AlGaAs/GaAs Cascade Cell Without AR Coating

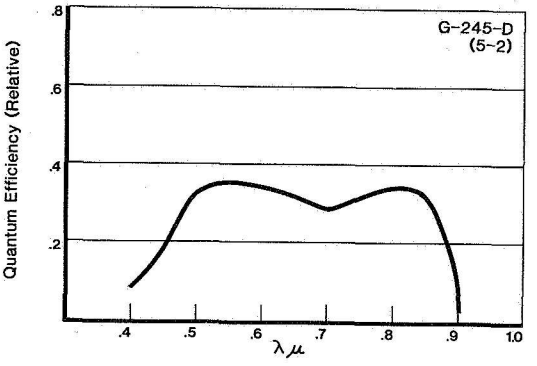

Figure 5. Spectral Response of AlGaAs/GaAs Cascade Solar Cell

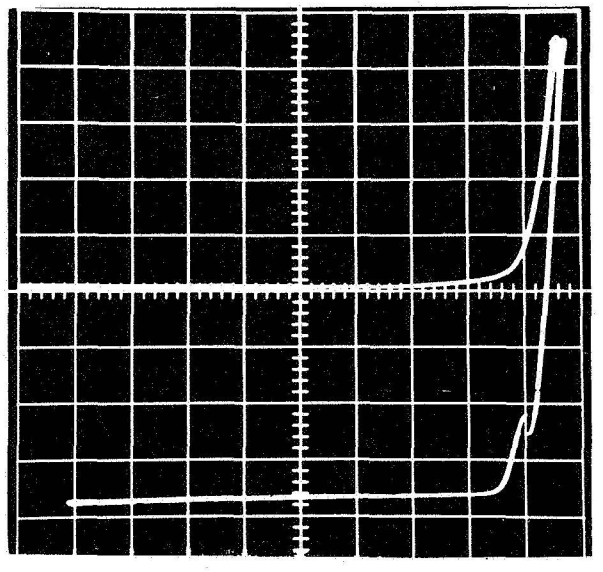

Figure 6. Effect of AlGaAs Tunnel Junction on the Characteristics of AlGaAs/GaAs Cascade Solar Cell at 30 suns AMO
Scale: 0.5 V/div Horizontal
0.1 mA/div Vertical